Movement-Aware Relay Selection for Delay-Tolerant Information Dissemination in Wildlife Tracking and Monitoring Applications

Yuhui Yao, Yan Sun, Chris Phillips, and Yue Cao, *Member, IEEE*

***Abstract*—As a promising use-case of the Internet of Things (IoT), wildlife tracking and monitoring applications greatly benefit the ecology-related research both commercially and scientifically. In literature, a forward-wait-deliver strategy has been researched to facilitate energy-efficient dissemination of delay-tolerant information, which penitentially contributes to long-term tracking and monitoring. However, this strategy is not directly applicable for wildlife tracking and monitoring applications, as the movement trajectory of animals cannot be precisely predicted for relay selection. To this end, further studies are required to utilize partially predictable mobility based on more generalized navigational information such as the movement direction. In this paper, the feasible exploitation of directional movement in path-unconstrained mobility is investigated for strategic forwarding. Our proposal is an advance to the state-of-the-art because the directional correlation of destination movement is considered to dynamically exploit the node mobility for the optimal selection of a stationary relay. Simulation results show that higher delivery utility can be achieved by the proposed fuzzy path model compared with a forwarding scheme without contact prediction or one based on linear trajectory model.**

***Index Terms*—Contact prediction, directional correlation, movement estimation.**

I. Introduction

As a PROMISING use-case of the Internet of Things (IoT), wildlife tracking and monitoring applications greatly benefit ecology-related research both commercially and scientifically [1]. With the deployment of numerous smart sensors/motes, remote close observation can be achieved on wild animals (e.g., deer [2], birds [3], fish [4], etc.) while unattended actions can be taken in a timely manner by automatic actuators (e.g., robotic drones [5]). Further accelerated by emerging technologies such as cloud computing [6] and machine-to-machine communication [7], these IoT applications will certainly provide an unprecedented panoramic view of the natural world.

Manuscript received February 26, 2018; revised April 9, 2018; accepted April 24, 2018. Date of publication April 30, 2018; date of current version August 9, 2018. *(Corresponding author: Yue Cao.)*

Y. Yao, Y. Sun, and C. Phillips are with the Department of Electronic Engineering and Computer Science, Queen Mary University of London, London E1 4NS, U.K. (e-mail: yuhui.yao@qmul.ac.uk; yan.sun@qmul.ac.uk; chris.i.phillips@qmul.ac.uk).

Y. Cao is with the Department of Computer and Information Sciences, Northumbria University, Newcastle upon Tyne NE1 8ST, U.K. (e-mail: yue.cao@northumbria.ac.uk).

Digital Object Identifier 10.1109/JIOT.2018.2831439

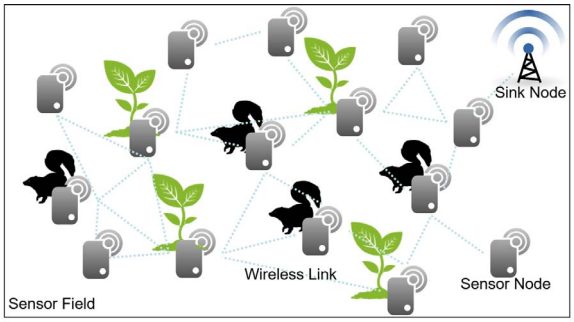

Fig. 1. Scenario example of wildlife tracking and monitoring applications.

Due to changing environments and requirements, it is a common need to reconfigure sensors and actuators (together referred as nodes in the remainder of this paper) from the sink (referred to as the gateway node which connects the rest of nodes with outside networks) [8]. To disseminate this configuration information (i.e., commands and updates), wireless multihop forwarding (called ad hoc networking) is a cost-effective solution when there is difficulty in directly reaching the target node, for instance, cases where there is limited communication capability or available infrastructure as is typical in the wild (such as forests and underwater). Via routes established between intermediate nodes, the whole network becomes reachable by the sink without relying on extra communication infrastructure (as shown in Fig. 1). Nevertheless, because the forwarding behavior is performed by resource-constrained wireless nodes, the energy efficiency of dissemination is a crucial issue to support long-term (months or years) tracking and monitoring.

In literature, a forward-wait-deliver (FWD) strategy has been adopted (such as [9]–[11]) to facilitate energy-efficient dissemination of delay-tolerant information. Instead of immediate delivery to the mobile destination, packets are forwarded to a relay[1] in advance, waiting for later delivery when the destination node is directly contactable. Given the movement trajectory reported by destination nodes (e.g., the vehicular navigation system), the FWD strategy can make full use of the possible delay budget to find an optimal forwarding route (usually by employing fewer hops as shown in Fig. 2), which

[1]The relay is selected from a set of nodes who are assumed to be temporarily or permanently stationary.

TABLE I
CLASSIFICATION OF MOBILITY DESCRIPTION FOR CONTACT PREDICTION WITH UNDERLYING MOVEMENT ESTIMATION

Type	Mobility Description	Movement Estimation	Contact Prediction	Example(s)
I	Complete travel plan	Defined waypoint model	Contactable locations (and the waiting time before contact)	[10] [11]
II	Explicit return period	Cyclic visit model	Contact interval (with/without uncertainty)	[13] [14]
III	Historical traces collection	Stochastic arrival model	Distribution of inter-contact time (and contact duration)	[15] [16]
IV	Value of estimated speed	Circular range model	Contactable area given delay	[17] [18]
V	Estimated speed with direction	Linear trajectory model	Expected contact location given delay	[19] [9]
VI	The diffusion exponent	Diffusive behaviour model	Contact likelihood given relative location	[20]

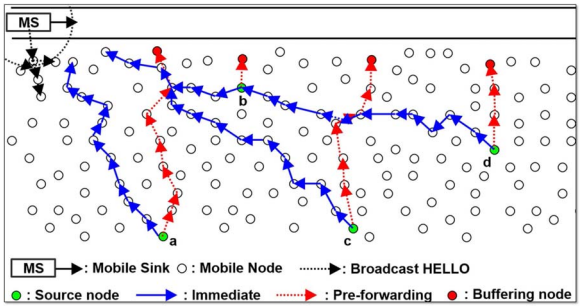

Fig. 2. Reduction of forwarding hops by FWD strategy [9].

is beneficial for reducing energy consumption and prolonging system lifetime. To make the problem more tractable, each delivery is assumed to be single-copied in this paper (i.e., no redundant copies are used to improve the possibility of successful delivery) while a multicopied scheme could be researched in future work.

With regard to the delay-tolerant configuration information (e.g., preplanned updates), the FWD strategy has the potential to bring the gain of dissemination efficiency. However, wildlife tracking and monitoring applications place high demand on deploying devices (attached or implanted) to animals, so the movement trajectory of these mobile nodes becomes less possible to be precisely predicted for relay selection. Meanwhile, animals usually move with a certain purpose (such as searching or migrating [12]) and therefore their movement reflects more-or-less predictability. To this end, further studies are required to utilize partially predictable mobility for adopting the FWD strategy based on more generalized navigational information such as the movement direction.

In this paper, the feasible exploitation of directional movement in path-unconstrained[2] mobility is investigated for strategic forwarding. The premise of our research is straightforward: a degree of persistence in the future direction of travel is expected on the basis of the current movement direction of a mobile node. As a consequence, there is a fair chance that a stationary node lying along this path will encounter the mobile node. Given adequate budget of delivery delay and enough confidence of movement persistence (i.e., the tendency to keep moving toward), the risk associated with opportunistic delivery probably can be balanced by the desire to reduce the number of forwarding hops. To the best of our knowledge, no existing research has provided such a quantitative analysis for strategic packet forwarding based on the comprehensive consideration of node mobility, network topology, and delivery requirements.

The main contribution of our research is a systematic framework for analytical modeling of relay selection.

1) Our proposal advances the state-of-the-art by considering the directional correlation of destination movement to dynamically exploit the node mobility for optimal selection of a stationary relay.
2) A novel fuzzy path model is proposed for movement estimation, where the influence of directional correlation is quantified by the standard deviation of turning angles.
3) By modeling of directional correlation, the proposed model provides more flexible estimation of directional movement within a path-unconstrained scenario where navigation systems are unavailable.

The rest of this paper is organized as follows. Section II introduces the related work to further demonstrate the research motivation and novelty. Sections III and IV provide the detailed system design and theoretical analysis. In Section V, simulation results are shown and the performance is discussed. This paper is finally concluded in Section VI.

II. RELATED WORK

This paper concerns the exploitation of node mobility for packet delivery. Among the state-of-the-art forwarding schemes, six types of mobility description for contact prediction are classified from the literature (as summarized in Table I). For these existing contact prediction schemes, the underlying movement estimation models are first discussed. Next, related studies on mobility modeling are reviewed, particularly in regard to the description and estimation of directional movement. Finally, a summary concludes the research novelty.

A. Modeling of Predictable Contact

For the ease of contact prediction, sufficient knowledge of node movement is usually assumed according to the first three types of mobility description listed in Table I. For the Type-I class, a complete travel plan is assumed to be known in advance and therefore future contactable locations can be directly predicted. Knowledge of predefined waypoints usually relies on access to the navigation system, for example to obtain a report of route information from vehicles, as assumed in [10] and [11]. For the Type-II class, although the knowledge of whole movement path is not required, strict periodicity is assumed in the contact interval (such as in [13] and [14]). For the Type-III class, the node mobility assumptions are further relaxed as a stochastic process. For instance, the invariant

[2]Mobile individuals independently move in relatively unobstructed environment (such as a forest or ocean).

properties of the intercontact time are discovered between vehicles and roadside units in [15] and [16]. However, stochastic properties can vary with cases and their analysis requires traces recorded over a long term and/or of a large quantity.

When the mobility knowledge is limited, the estimation of node movement plays an important role in contact prediction. For the last three types listed in Table I, the latest location of the mobile node is taken as the reference point and the contact is predicted by estimating the node movement. For the Type-IV class, a maximum (or average) movement speed is estimated for the mobile node, so a circular movement range can be drawn to predict contact (as in [17] and [18]), where the radius depends on the delay since the location report. For the Type-V class, with additional knowledge on movement direction, the location of future contact can be expected given the delay (such as in [9] and [19]). However, the speed and direction are not enough to differentiate heterogeneous mobility, which limits the contact prediction based on the Type-IV/V mobility description. For the Type-VI class, a diffusion constant is introduced by [20] based on the exponent parameter of the step-length distribution in Lévy walk model. Compared with the movement speed, the diffusion constant is a better characterization of diffusive behavior, as the randomness of step length is taken into consideration. Nevertheless, to the best of our knowledge there remains no prior work that considers differentiation of directional movement for contact prediction.

B. Modeling of Directional Movement

Unlike the completely unpredictable movement imitated by memoryless random mobility, mobile nodes tend to move smoothly in many cases and sharp turns rarely occur [21]. To reflect this directional movement behavior, correlated motion patterns are researched in the literature. The existing patterns for directional correlation can be roughly divided into two branches: 1) velocity-based or 2) step-based. For the first branch, correlation patterns focus on the gradual change of velocity which leads to the persistence in movement direction. In [22], the degree of temporal correlation is governed by a memory level parameter, but difficulty arises from controllable correlation of movement direction because the velocity component in each spatial dimension is independently modeled as a Gauss–Markov process. In [23], despite the modeling of accelerations, the probability in choosing movement direction is basically isotropic because the authors purely focus on dividing changes into several small increments. In contrast, the correlation patterns in the second branch are based the characterization of step direction. In [24] and [25], the directional correlation between random steps is investigated but their research is restricted to an n-dimensional lattice or grid. In [26], the directional preference of random step is described by a probability distribution model, but an additional assumption is required for fixing a bias of movement direction. In [27], the angle of maximum turn is introduced to bound the random turning angle (RTA), which results in a directional correlation between steps. However, the influence of RTA in movement is not analyzed by [27] or any later reference, as their focus is on the network simulation rather than movement analysis.

From the biophysics-related fields, further studies on the RTA are found concerning the correlated random walk (CRW) model [28]. In [29], circular distribution functions are employed as the model of RTA, which is theoretically rigorous but introduces additionally complexity. In [30], both the angle of maximum turn and the standard deviation of the turning angles (SDTAs) are considered to characterize the probability distribution of RTA. In [31], the probability distribution model of RTA is linked to the diffusion degree to analyze the movement of animals. For the aforementioned research on CRW, the distance-based metrics, such as the mean square displacement, have been commonly analyzed and formulated. However, the calculative method to estimate the displacement angle based on the distribution characteristics of RTA cannot be found from the literature. Furthermore, to the best of our knowledge, none of existing works include a formal discussion regarding a truncated distribution model for RTA.

C. Summary

The above literature review suggests that the state-of-the-art (as classified in Table I) is insufficient to reasonably predict contact caused by directional movement. By introducing directional correlation as an index of node mobility, predictable contact can be extended to facilitate strategic forwarding, although problems remain unsolved in terms of characterization and exploitation. From an analytical modeling perspective, our proposal is described in Section III with further analysis provided in Sections IV and V.

III. System Model

In the previous sections, the role of mobility analysis and how it can be exploited has been considered. To overcome the remaining challenge of exploiting directional movement in path-unconstrained mobility, an analytical framework (with key notations listed in Table II) is proposed in this section and is elaborated from three aspects. First, the correlation pattern of node mobility is considered to represent directional movement. Second, based on the mobility model, contact opportunities are mathematically analyzed as a stochastic process. Finally, the delivery utility is defined and analyzed.

A. Mobility Model

Devising a suitable mobility model is the first step in creating a successful dynamic delivery mechanism. Without loss of generality, we consider a mobile target moves within a 2-D space $\mathbb{R}^2$.

The fluctuations of movement speed are assumed to be negligible compared with the mean value, so that the average speed (denoted by V) is considered to be a constant as

$$V = v(t) - \Delta v(t) \approx v(t) \tag{1}$$

TABLE II
LIST OF KEY NOTATIONS

Notation	Explanation
V	the average movement speed
T	the duration of a step period
θ	the movement direction
Θ	the random turning angle between successive steps
λ_i	the movement distance during step i
ω_i	the movement direction during step i
$\vec{e}_i$	the displacement vector after i steps
R	the radius of contact range
n_j	a stationary node
$\mathcal{N}$	the whole set of stationary nodes
d_j	the distance from n_j to the mobile target
$\vec{e}_j$	the relative position coordinates of n_j
H_j	the forwarding hops from the gateway node to n_j
m_k	a task of delivery from the gateway to a mobile destination
$\mathcal{M}$	the whole set of delivery tasks
M	the total number of delivery tasks
B_k	the delay budget of m_k
h_k	the minimum hop number for m_k
c_k	the forwarding cost for m_k
s_k	the expected satisfactory degree of delivery
τ, τ_k	a upper bound of step number (given B_k)
μ, μ_τ	the certainty degree of contact (within step bound τ)
η	a threshold of certainty degree
$\mathcal{N}_{\tau,\eta}$	the subset of stationary nodes considered as the movement path of the mobile target given τ and η
$\mathcal{N}_k$	the qualified candidates of stationary nodes for m_k
u	the delivery utility as the ratio of overall satisfactory degree to the overall forwarding cost

where $v(t)$ denotes the movement speed at time point t and $\Delta v(t)$ denotes the speed variation from the average at time point t.

The movement direction (denoted by $\theta \in [-\pi, \pi]$) is assumed to be fixed during a step which is a constant period defined as

$$T = t_{i+1} - t_i \tag{2}$$

where $i \in \mathbb{N}$ denotes the discrete step number corresponding to the time point t_i.

Between two successive steps, the movement direction is updated by an angle of random turning

$$\Theta_i = \theta_i - \theta_{i-1} \tag{3}$$

where θ_i denotes the movement direction during time step i, and $\Theta_i \in [-\pi, \pi]$ denotes the RTA between steps $i-1$ and i.

For the movement made during the i time step, λ_i denotes the step movement distance and ω_i denotes the step movement direction. Based on (1)–(3), the step movement distance and direction can be derived as

$$\lambda_i = V \cdot T \tag{4}$$

$$\omega_i = \theta_i = \theta_{i-1} + \Theta_i. \tag{5}$$

Given an initial movement direction (denoted by θ_0), (5) can be further rewritten as

$$\omega_i = \theta_0 + \sum_{\zeta=1}^{i} \Theta_\zeta. \tag{6}$$

Consequently, the real-time movement of a mobile target can be specified given the initial direction and the probability distribution of the RTAs. Under such a mobility model, the persistence of the initial movement direction progressively diminishes over successive time steps, which will be further discussed in Section IV.

B. Contact Model

Having described the mobility model, we now turn our attention to the modeling of contact. A traditional model of unit disk [32] is considered where there is a constant radius of contact range (denoted by R). Let $\mathcal{N}$ denote the whole set of stationary nodes, then a stationary node (denoted by n_j) is contactable by the mobile object if only if

$$d_j(i) \le R \tag{7}$$

where $d_j(i)$ denotes the distance between n_j and the mobile target as a function of step number i.

The certainty degree of contact (denoted by $\mu \in [0, 1]$) between the mobile target and n_j within finite steps can be described as

$$\mu_\tau(n_j) = \Pr\big[\min\big(d_j(i)\big) \le R \mid i \le \tau\big] \tag{8}$$

where $\tau \in \mathbb{N}$ denotes a bound of step number, and μ_τ denotes a function of certainty degree which is dependent on $d_j(i)$ given τ.

Taking (8) as the membership function, a fuzzy set of the stationary nodes is defined as

$$\mathcal{N}_{\tau,\eta} = \big\{n_j \mid \mu_\tau(n_j) \ge \eta\big\} \tag{9}$$

where $\eta \in [0, 1]$ denote a threshold of certainty degree and $\mathcal{N}_{\tau,\eta}$ denotes the subset of stationary nodes considered to be along the movement path of the mobile target given τ and η.

To calculate $d_j(i)$, a polar coordinate system is considered where r denotes the relative distance from the original position of the mobile target, and φ denotes the relative angle measured with respect to the initial movement direction of the mobile target. The localization and tracking techniques can be referred from works such as [33]. Under such coordinate system, the position coordinates of the mobile target after i steps (denoted by $\vec{e}_i$) and the position coordinates of n_j (denoted by $\vec{e}_j$) can be respectively described as

$$\vec{e}_i = (r_i, \varphi_i) \tag{10}$$

$$\vec{e}_j = \big(r_j, \varphi_j\big). \tag{11}$$

According to the law of cosines in trigonometry

$$\begin{aligned} d_j(i) &= \big|\vec{e}_i - \vec{e}_j\big| \\ &= |\vec{e}_i|^2 + \big|\vec{e}_j\big|^2 - 2|\vec{e}_i|\big|\vec{e}_j\big| \cdot \cos\langle\vec{e}_i, \vec{e}_j\rangle \\ &= r_i^2 + r_j^2 - 2r_i r_j \cdot \cos\big(\varphi_i - \varphi_j\big). \end{aligned} \tag{12}$$

The r_j and φ_j are known constants given the original position and the initial movement direction of the mobile target. However, due to the RTA as described in (3), $\vec{e}_i$ is a stochastic process as $\{(r_i, \varphi_i) : i \in \mathbb{N}\}$, where r_i and φ_i are random variables representing the displacement distance and angle observed after i steps, respectively. To quantify the contact potential, this movement process is further analyzed in Section IV.

C. Strategy Model (Design of Forward-Wait-Deliver)

Based on the predictable contact, strategies can be made for efficient forwarding. Let m_k denotes the task of delivering a data item from the gateway node to a mobile destination node, and a whole set of tasks is denoted by $\mathcal{M}$. In this paper, we assume these delivery tasks are independent, which represents a generalized scenario that can be either a delivery to a whole group of destinations or separate deliveries to a single destination. The strategy of relay sharing for group delivery, as in [10], is left for future work. Considering delivery tasks of different importance is also beyond the scope of this paper.

For the delivery with delay tolerance, predictable contact can be considered in order to reduce the number of transmissions. Let B_k denote the delay budget of m_k, then corresponding maximum allowed step number (denoted by τ_k) can be calculated as

$$\tau_k = \left\lfloor \frac{B_k}{T} \right\rfloor. \tag{13}$$

Thus, for example, if the delay budget is 1300 s and the step period is 200 s then there are six permitted steps.

As with the delivery scheme considered in [10], packets are first sent to the selected stationary relay nodes by multihop forwarding for later last-hop delivery. Then the delivery is accomplished by the stationary relay node when the mobile destination node is directly contactable. Based on the fuzzy set defined by (9), qualified candidate stationary nodes for m_k can be defined as

$$\mathcal{N}_k(\eta) = \left\{ n_j \mid \mu_{\tau_k}(n_j) \geq \eta \right\}. \tag{14}$$

As the stationary nodes form a fixed network topology, we assume knowledge of forwarding hops from the gateway node to any stationary node n_j is available at the gateway node, which is denoted by H_j. For each delivery, the stationary node with the least forwarding hops is selected from the candidates as

$$h_k(\eta) = \min_{n_j \in \mathcal{N}_k(\eta)} \left(H_j \right) \tag{15}$$

where $h_k(\eta)$ denotes the minimum hop number for m_k given η.

Without considering retransmission and duplication issues, transmission consumed energy is primarily proportional to the number of forwarding hops. As the final hop from the relay to the destination should be counted as well, the forwarding cost for m_k is defined as

$$c_k(\eta) = 1 + h_k(\eta) \tag{16}$$

where the plus one counts for the expected last-hop delivery.

As defined by (14), any stationary node selected from $\mathcal{N}_k(\eta)$ guarantees the certainty degree η for on-time contact with the mobile destination. Ideally, a successful contact has the direct contribution to final delivery and therefore the satisfactory degree of delivery is expected as

$$s_k(\eta) = \eta \tag{17}$$

where $s_k(\eta)$ denotes the expected satisfactory degree of delivery given η.

Finally, the delivery utility is considered as a metric to assess the efficiency of the completion of the whole set of delivery tasks. As the ratio of overall satisfactory degree to the overall forwarding cost, the delivery utility (denoted by u) is defined as

$$\begin{aligned} u(\eta) &= \frac{\sum_{m_k \in \mathcal{M}} s_k(\eta)}{\sum_{m_k \in \mathcal{M}} c_k(\eta)} \\ &= \frac{M \cdot \eta}{M + \sum_{m_k \in \mathcal{M}} h_k(\eta)} \\ &= \frac{\eta}{1 + h_{\text{avg}}(\eta)} \\ &\leq \frac{\eta}{1 + h_{\min}(\eta)} \end{aligned} \tag{18}$$

where $u(\eta)$ denotes the achievable utility given η, M denotes the total number of delivery tasks, $h_{\text{avg}}(\eta)$ denotes the average forwarding hops over all the deliveries, and $h_{\min}(\eta)$ denotes the minimum forwarding hops for single delivery.

The utility value reflects the satisfactory degree contributed by each forwarding hop for the whole set of delivery tasks. Equation (18) shows that the delivery utility is dependent on the certainty threshold η and is related to the average forwarding hops. Although the direct optimization of delivery utility is impossible as it requires analysis on a case-by-case basis, (18) shows that the maximum of utility value is bounded by the minimum forwarding hops for single delivery. Consequently, it is possible to realize a higher achievable utility by adjusting η, as a lower threshold of required certainty can provide more candidates and therefore the minimum hop number of forwarding tends to decrease. To explore this possibility, further analysis and simulation are conducted in Section V.

IV. Contact Modeling From Directional Movement

A. Directional Correlation

In Section III, an analytical framework is provided for exploiting mobility in strategic forwarding. Based on the mobility model, the predictable contact with a mobile target can be utilized to select relay(s) from a set of stationary nodes. However, because the movement direction changes randomly in a correlated pattern, it is not easy to obtain a simple expression of the contact potential. To this end, further analysis is required on the stochastic process of movement.

As assumed in (1)–(3), the uncertainty of movement results from the RTA between two successive steps. In Fig. 3, a comparison is shown between three types of distribution for RTA. Traditionally, it is assumed that the current movement direction may change to any other direction with equal probability. This uncorrelated change can be represented by an isotropic uniform distribution. By restricting the maximum allowed direction change, the bounded uniform distribution [27] leads to correlation in the step direction. However, this bounded uniform distribution fails to reflect the natural phenomenon that smaller deviations tend to have higher frequency of occurrence. Therefore, in this paper, the truncated normal distribution is proposed as the probability model for RTA.

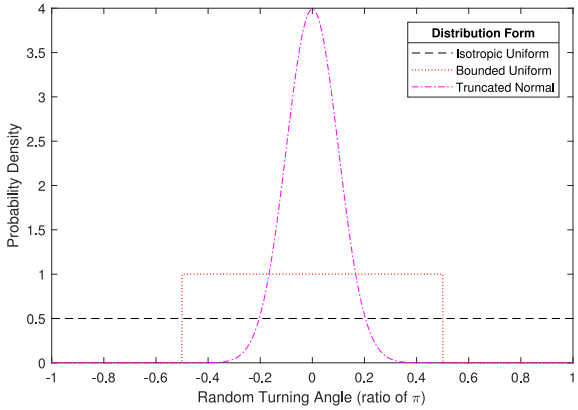

Fig. 3. Comparison between three types of probability distribution.

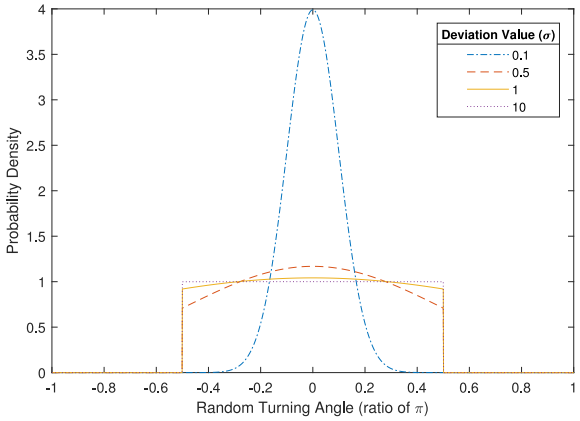

Fig. 4. Effect of deviation value on the truncated normal distribution.

Based on the zero-centered normal distribution with symmetric truncation, the probability density of the RTA is given as

$$\Pr[\Theta = \delta] = \frac{\phi\left(\frac{\delta}{\sigma}\right)}{\sigma\left(2\Phi\left(\frac{\epsilon}{\sigma}\right) - 1\right)} \tag{19}$$

where ϕ and Φ denote the probability density function and cumulative distribution function of the standard normal distribution, respectively. $\sigma > 0$ denotes the standard deviation, $\epsilon \in [0, \pi]$ denotes the truncation bound, and Θ denotes the RTA as defined in (3).

Then the probability of a turning angle within a given interval can be expressed as

$$\Pr[l_1 \le \Theta \le l_2] = \frac{\Phi\left(\frac{l_2}{\sigma}\right) - \Phi\left(\frac{l_1}{\sigma}\right)}{2\Phi\left(\frac{\epsilon}{\sigma}\right) - 1} \tag{20}$$

where $-\pi \le l_1 < l_2 \le \pi$ denote the two ends of the interval.

Due to the truncation, the probability is zero outside the bounded range, which can be proved as

$$\begin{aligned}\Pr[\epsilon < |\Theta| \le \pi] &= 1 - \Pr[-\epsilon \le \Theta \le \epsilon] \\ &= 1 - \frac{\Phi\left(\frac{\epsilon}{\sigma}\right) - \Phi\left(\frac{-\epsilon}{\sigma}\right)}{2\Phi\left(\frac{\epsilon}{\sigma}\right) - 1} \\ &= 1 - \frac{\Phi\left(\frac{\epsilon}{\sigma}\right) - \left(1 - \Phi\left(\frac{\epsilon}{\sigma}\right)\right)}{2\Phi\left(\frac{\epsilon}{\sigma}\right) - 1} \\ &= 0. \end{aligned} \tag{21}$$

Meanwhile, the effect of truncation depends on the relative relationship between σ and ϵ. As shown in Fig. 4, the possible turning angle is represented as a random variable having a continuous distribution between truncation bounds. Given a certain truncation bound ϵ, the shape of distribution curve varies with the value of σ. With an increasing σ value, the density difference within the bounded range becomes smaller. For the special case that σ is extremely large, a uniform distribution is approximated.

When the value of σ is sufficiently small compared with the truncation bound ϵ, the truncated normal distribution is very close to a normal distribution without truncation. To measure the relationship between σ and ϵ, we define a ratio as

$$\rho = \frac{\epsilon}{\sigma}. \tag{22}$$

Then (19) can be written as

$$\begin{aligned}\Pr[\Theta = \delta] &= \frac{\phi\left(\frac{\delta}{\sigma}\right)}{\sigma(2\Phi(\rho) - 1)} \\ &\approx \frac{\phi\left(\frac{\delta}{\sigma}\right)}{\sigma} \qquad \rho \ge \rho_{\text{th}}\end{aligned} \tag{23}$$

where ρ_{th} is a threshold value that satisfies $\Phi(\rho) \approx 1$ and typically $\rho_{\text{th}} \ge 4$.

With the condition $\rho \ge \rho_{\text{th}}$, the truncated normal distribution can be simplified such that it is only affected by the single parameter σ which stands for the SDTAs in this paper. In other words, the normal distribution is considered naturally bounded within a certain range. To apply this single-parameter description, the maximum allowed value of σ is given as

$$\sigma_{\max} = \frac{\epsilon_{\max}}{\sigma_{\min}} = \frac{\pi}{\rho_{\text{th}}}. \tag{24}$$

B. Movement Estimation

As described in Section III, the prediction of contact is dependent on the estimation of movement, which the key of strategy making. Here, the stochastic properties are further analyzed to estimate the movement.

Based on (4) and (5), the displacement distance projected on the axial direction can be given as

$$r_i \cdot \sin\varphi_i = \sum_{\zeta=1}^{i}(\lambda_i \cdot \sin\omega_i) = V \cdot T \cdot \sum_{\zeta=1}^{i}\left(\sin\omega_\zeta\right). \tag{25}$$

Similarly, the displacement distance projected on the radial direction can be given as

$$r_i \cdot \cos\varphi_i = V \cdot T \cdot \sum_{\zeta=1}^{i}\left(\cos\omega_\zeta\right). \tag{26}$$

Dividing (25) by (26), we obtain

$$\tan\varphi_i = \frac{\sum_{\zeta=1}^{i}\left(\sin\omega_\zeta\right)}{\sum_{\zeta=1}^{i}\left(\cos\omega_\zeta\right)}. \tag{27}$$

TABLE III
SYNTHETIC TRACES GENERATION FOR MONTE CARLO EXPERIMENTS

Parameters	Values
Truncation Bound	$\pm\pi$
ρ_{th}	4
σ (SDTA)	5,10,15,20,25,30,35,40,45 (degrees)
Movement Speed	1 m/s
Initial Direction	x-axis positive direction
Original Position	central point (0,0)
Step Period	30 seconds
Observation Period	3600 seconds
Number of Traces	10000 for each SDTA value

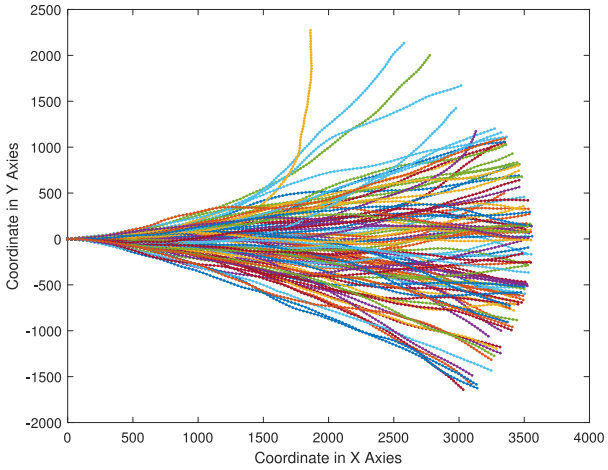

Fig. 5. 100 traces generated by setting SDTA to 10°.

Consequently,

$$\varphi_i = \arctan\left(\frac{\sum_{\zeta=1}^{i}\left(\sin\left(\theta_0 + \sum_{\xi=1}^{\zeta}\Theta_\xi\right)\right)}{\sum_{\zeta=1}^{i}\left(\cos\left(\theta_0 + \sum_{\xi=1}^{\zeta}\Theta_\xi\right)\right)}\right) \tag{28}$$

where φ_i denotes the displacement angle after i steps.

Due to the complexity of (28), the probability distribution of φ_i cannot be solved directly. However, according to the central limit theorem [34], independent and identically distributed random variables tend toward the normal distribution. Therefore, the distribution of the displacement angle after a number of steps is expected to be a bell-shape curve given as

$$f_{\text{Gauss}}(z) = \alpha \cdot \exp\left(-\left(\frac{z-\beta}{\gamma}\right)^2\right) \tag{29}$$

where f_{Gauss} denotes the Gaussian function, z denotes the independent variable, α denotes the amplitude factor, β denotes the centroid factor, and γ denotes the scale factor.

Based on the Monte Carlo method [35], simulation experiments are conducted to confirm the validity of distribution and to obtain the model parameters. Given initial parameters[3] (specified in Table III), a set of synthetic traces can be generated as shown in Fig. 5. A clearer view can be provided by sampling the trace points only at the selected steps as shown in Fig. 6.

As shown in Fig. 7, the frequency of a particular displacement angle is counted at each sampled step. The statistical

[3]Settings in this paper are based on the normal walking behaviors but scalable to other scenarios.

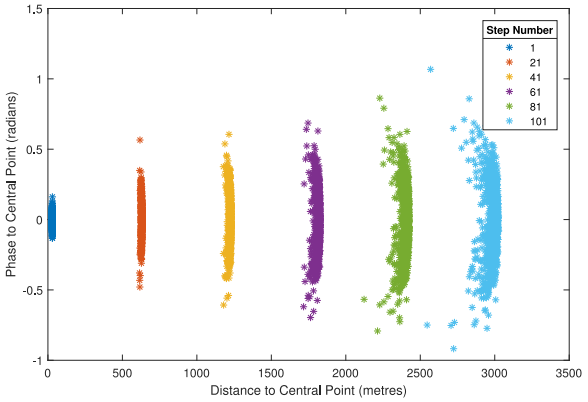

Fig. 6. Trace points sampled at selected steps from 1000 traces (setting SDTA to 10°).

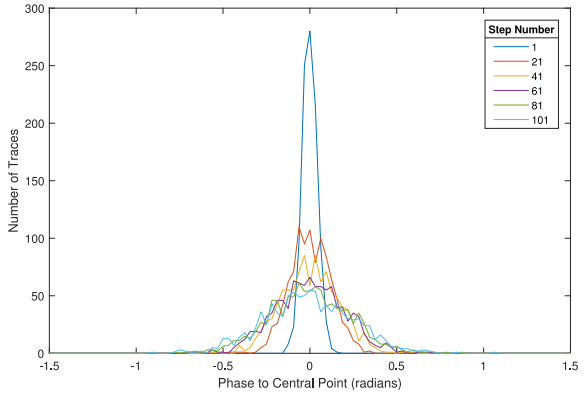

Fig. 7. Frequency statistics of displacement angle sampled at selected steps from 1000 traces (setting SDTA to 10°).

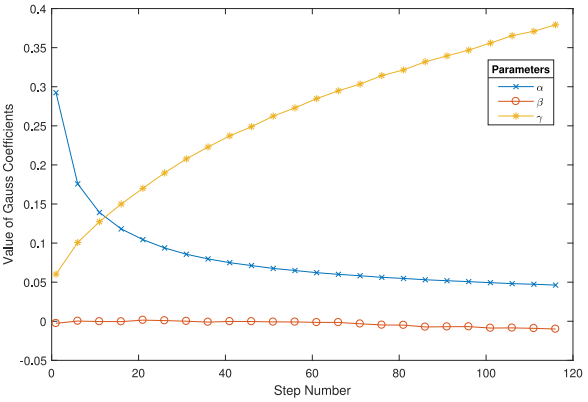

Fig. 8. Fitted model parameters at different step numbers (setting SDTA to 10°).

results visually show a trend toward the normal distribution. By fitting the simulated frequency distribution of each sampled step to the bell-shape curve given in (29), functional relationships are reflected between the three model parameters and the step numbers. As shown in Fig. 8, the amplitude factor decreases and the scale factor increases nonlinearly with increasing step number, whilst the centroid factor remains constant. With the "NonlinearLeastSquares" fitting method and "Trust-Region" fitting algorithm provided by the MATLAB

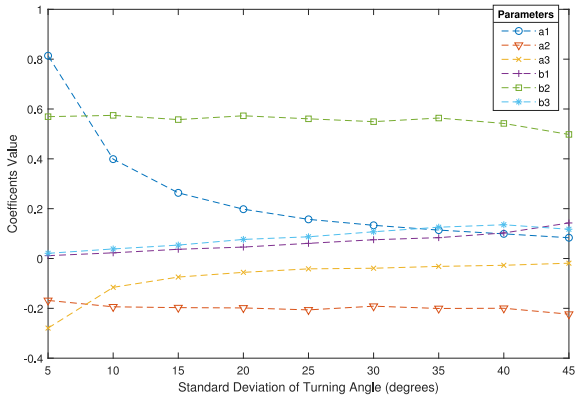

Fig. 9. Further fitted model parameters at different SDTA values.

curve fitting toolbox, the factor relationships are obtained as

$$\begin{cases} \alpha = a_1 \cdot i^{a_2} + a_3 \\ \beta = 0 \\ \gamma = b_1 \cdot i^{b_2} + b_3 \end{cases} \tag{30}$$

where α, β, and γ are the three factors defined in (29), a_1, a_2, a_3, b_1, b_2, and b_3 are parametric constants, and i denotes the step number.

As shown in Fig. 9, further fitting the parameters obtained in (30), the relationships can be found with the SDTA. Using the same fitting technique, the parameter relationships are obtained as

$$\begin{cases} a_1 = p_1 \cdot \sigma^{p_2} \\ a_2 = p_3 \\ a_3 = p_4 \cdot \sigma^{p_5} \\ b_1 = p_6 \cdot \sigma + p_7 \\ b_2 = p_8 \\ b_3 = p_9 \cdot \sigma + p_{10} \end{cases} \tag{31}$$

where a_1, a_2, a_3, b_1, b_2, and b_3 are parametric constants defined in (30), p_1–p_{10} are fitting parameters, and σ denotes the SDTA.

Based on (29)–(31), the curve shape can be defined as a parametric model

$$\begin{cases} f_{\text{shape}}(z, \sigma, i) = \alpha(\sigma, i) \cdot \exp\left(-\left(\frac{z-\beta}{\gamma(\sigma,i)}\right)^2\right) \\ \alpha(\sigma, i) = (p_1 \cdot i^{p_2}) \cdot \sigma^{p_3} + (p_4 \cdot i^{p_5}) \\ \gamma(\sigma, i) = (p_6 \cdot i + p_7) \cdot \sigma^{p_8} + (p_9 \cdot i + p_{10}) \\ \beta = 0 \end{cases} \tag{32}$$

where f_{shape} denotes the curve shape function, z denotes the independent variable, σ denotes the SDTA, i denotes the step number, and p_1 to p_{10} are parameters (listed in Table IV) solved under Table III configurations.

Then the probability distribution function of displacement angle after certain steps (denoted by f_{pdf}) can be obtained as

$$\Pr[\varphi_i = \delta] = f_{\text{pdf}}(\delta, \sigma, i) = \frac{f_{\text{shape}}(\delta, \sigma, i)}{\int_{-\pi}^{\pi} f_{\text{shape}}(z, \sigma, i) dz}. \tag{33}$$

As shown in (33), the probability distribution of displacement angle varies over steps and is dependent on SDTA. This distribution model provides a tool to quantify the directional movement, which will be applied in Section IV-C for contact prediction.

TABLE IV
SOLVED MODEL PARAMETERS

Parameters	Values	Parameters	Values
p_1	0.0675	p_6	0.1694
p_2	-1.0207	p_7	-0.0092
p_3	-0.1976	p_8	0.5542
p_4	-0.0157	p_9	0.1627
p_5	-1.1786	p_{10}	0.0137

C. Contact Prediction

In Section IV-B, a parametric model is proposed to estimate the displacement angle over steps based on the SDTAs. Now, we apply this estimation model in an three-phases approach to describe the contact certainty based on the relative distance (denoted by r) from the original position of the mobile target, and the relative angle (denoted by φ) measured with respect to the initial movement direction of the mobile target.

For the first phase, an estimated step number (denoted by i_{est}) is calculated as

$$i_{\text{est}} = \frac{r}{V \cdot T} \tag{34}$$

where V denotes the average speed and T denotes the step period.

For the second phase, the range of directional coverage is given as

$$\left[\varphi_{\min}^{\text{cover}}, \varphi_{\max}^{\text{cover}}\right] \tag{35}$$

$$\varphi_{\min}^{\text{cover}} = \varphi - \sin\left(\frac{R}{r}\right) \tag{36}$$

$$\varphi_{\max}^{\text{cover}} = \varphi + \sin\left(\frac{R}{r}\right) \tag{37}$$

where $\varphi_{\min}^{\text{cover}}, \varphi_{\max}^{\text{cover}} \in [-\pi, \pi]$ denotes the minimum/maximum coverage angle and R denotes the radius of contact range.

For the third phase, the contact certainty (denoted by μ_{est}) is finally described as

$$\begin{aligned} \mu_{\text{est}} &= \Pr\left[\varphi_{\max}^{\text{cover}} \geq \varphi_{i_{\text{est}}} \geq \varphi_{\min}^{\text{cover}}\right] \\ &= \int_{\varphi_{\min}^{\text{cover}}}^{\varphi_{\max}^{\text{cover}}} f_{\text{pdf}}(\delta, \sigma, i_{\text{est}}) d\delta \\ &= f_\sigma(r, \varphi) \end{aligned} \tag{38}$$

where f_σ denotes the estimation function given σ.

Thus, the contact certainty is formulated as a spatial distribution given SDTA. This distribution model describes statistically predictable contact with spatial points, which is later applied for the selection of stationary relay node. With configurations specified by Table V, a simulation is first conducted to visually demonstrate this distribution model.

As shown in Fig. 10, the geographical region is equally divided into multiple grids, where the mobile node is originally located at the central grid point with initial movement direction toward the x-axis positive direction. Based on (38), the contact certainty is estimated for each grid point given SDTA. The results show that this model can reflect the decreasing

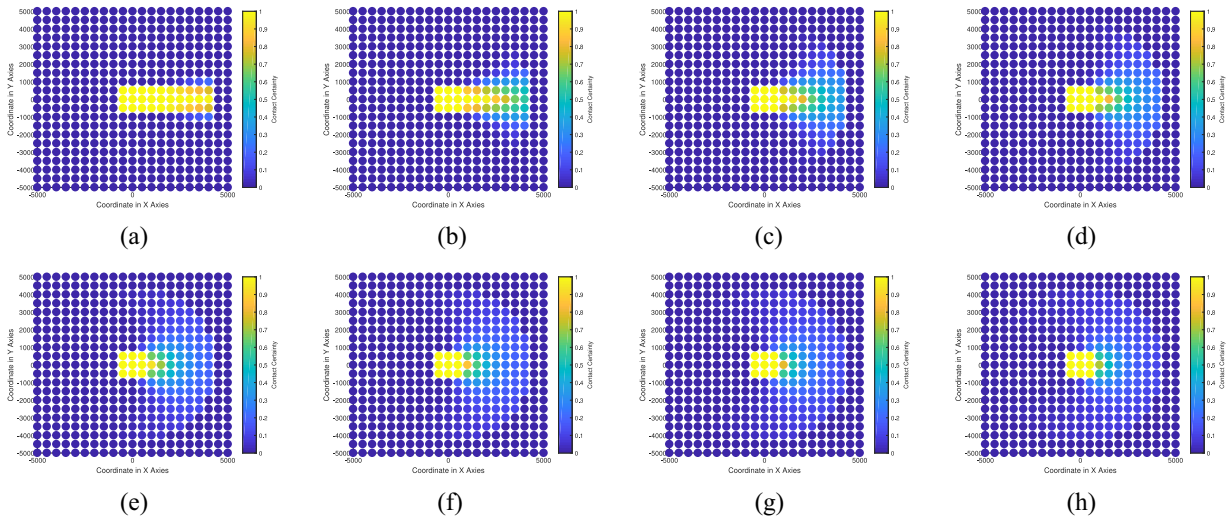

Fig. 10. Spatial distribution of contact certainty based on the estimation model for different values of SDTA. (a) 5°. (b) 10°. (c) 15°. (d) 20°. (e) 25°. (f) 30°. (g) 35°. (h) 40°.

TABLE V
SIMULATION CONFIGURATIONS FOR CONTACT PREDICTION

Parameters	Values
Mobility Configurations	Same with Table III
Model Parameters	Same with Table IV
Region Size	10000*10000 metres
Grid Size	500*500 metres
Radius of Contact Range	750 metres

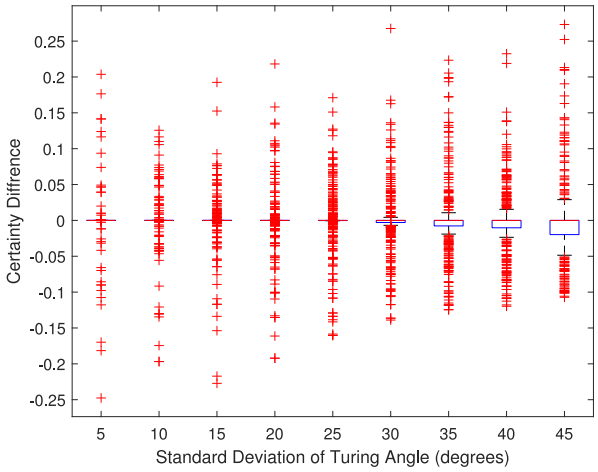

Fig. 11. Box plot of certainty difference for the accuracy validation.

predictability with increasing value of SDTA (i.e., the less directional correlation). The varying predictability does not affect the central nine grid points because they are directly contactable and no estimation is required.

To further validate the model accuracy, test traces are generated synthetically (100 traces for each SDTA value with same parameters listed in Table III). The ratio of contactable traces is calculated for each grid point as the tested contact certainty. The certainty difference is defined as the tested certainty minus the estimated certainty, so a positive difference value reveals an underestimate and a negative difference value reveals an overestimate. In Fig. 11, the certainty difference at each grid points

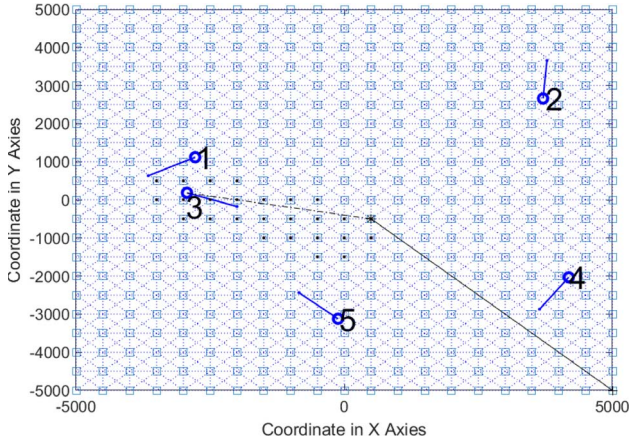

Fig. 12. Illustrated delivery solution for the third of five tasks (based on the linear trajectory model by setting delay budget to 3000 s).

is shown for different SDTA values. Because (38) is not an accurate calculation of contact probability, either underestimation or overestimation may exist as the results show. However, it can be observed the model can adaptively react to the varying SDTA so that the difference values are mostly bounded by 0.1 and the rare extreme values are roughly bounded by 0.25. As a conclusion, the approximate estimation model can reflect the effect of directional correlation on contact certainty.

V. CONTACT MODELING FOR RELAY SELECTION

In Section III, a mathematical analysis on strategy model reveals the possibility of higher achievable utility by adjusting the threshold of contact certainty in stationary relay node selection. Now, we further explore its practical effect in a simulation scenario (configurations specified by Table VI).

As shown in Fig. 12, a rectangular region is considered as the network area where a certain number of stationary nodes (denoted by blue squares) are uniformly deployed. Single-hop connectivities (denoted by blue dashed lines) exist between

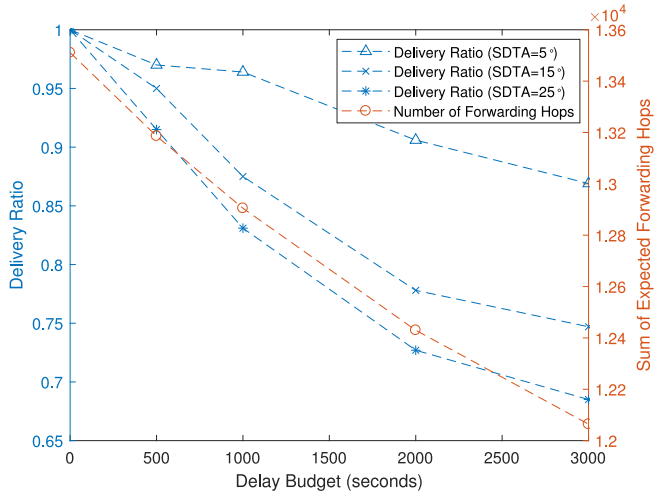

Fig. 13. Effect of delay budget on linear trajectory model.

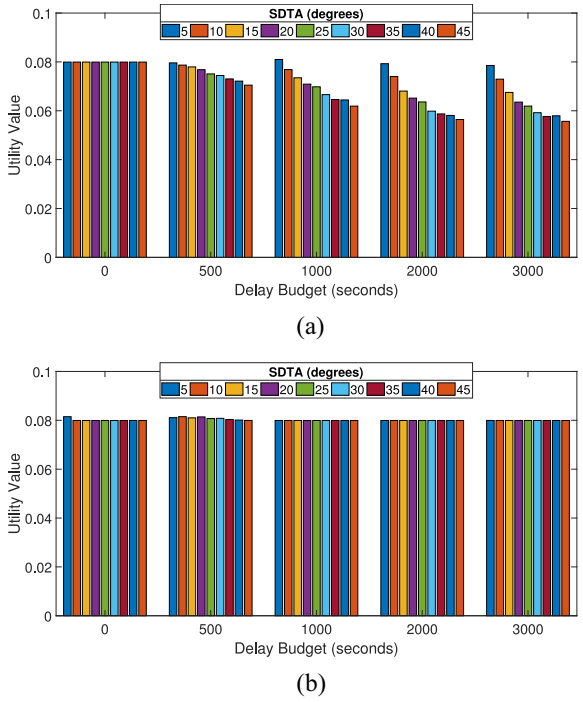

Fig. 14. Comparison of delivery utility for different values of delay budget and SDTA. (a) Linear trajectory model. (b) Fuzzy path model.

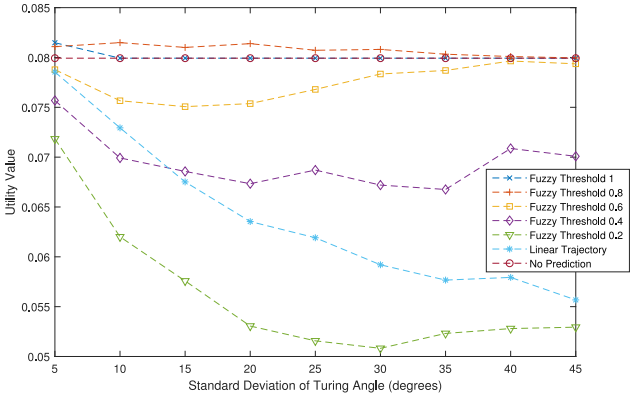

Fig. 15. Comparison of delivery utility for different values of SDTA (setting delay budget to 3000 s).

neighboring stationary nodes, which form a grid network topology. One of the stationary nodes (located at the bottom right corner in our case) serves as the gateway node which connects to the outside of network area. A certain number of delivery tasks are to be accomplished, where all the deliveries come from the gateway node and each goes to a mobile destination node. The original position (denoted by a blue circle) and initial movement direction (denoted by a blue solid line) of the mobile destination node are randomly and independently decided for each delivery task.

To accomplish a delivery task, one stationary node is selected from a set of candidates (denoted by black dots) as the last-hop relay. The selected stationary relay node (denoted by a black asterisk) is responsible for the direct delivery when the mobile destination node is contactable. Based on the network topology formed by stationary nodes, the gateway node connects to the selected stationary relay node by a multihop forwarding route. The position-based unicast routing is considered for packet forwarding due to its low computation and communication overhead [36]. In Fig. 12, the black solid line shows the multihop forwarding route and the black dashed-dotted line indicates the expected contact with the mobile destination node. By selecting the stationary node with the fewest possible forwarding hops as the relay node, the transmission times can be reduced which is beneficial for prolonging network lifetime. Thus, the remaining problem is listing candidates from stationary nodes based on the mobility information.

In Figs. 13 and 14, we show the limitation of a linear trajectory model and how our proposed fuzzy path model overcomes it. To evaluate the performance of relay selection, synthetic traces are generated (one trace for each delivery task) and the trace generation is repeated for different SDTA values (referring Table III). For delivery without delay tolerance (i.e., delay budget equals to zero in Fig. 13), the stationary relay node is selected from the immediate neighboring nodes identified given the latest position of the mobile node. With increasing budget of delivery delay (500, 1000, 2000, and 3000 s in Fig. 13), more stationary nodes can be listed as candidates by predicting contact based on linear trajectory model and therefore the number of forwarding hop can be reduced. However, the delivery ratio[4] will decrease at the same time, which worsens with higher SDTA because of the lower persistence of directional movement. Consequently, the delivery utility [as defined in (18)] will decrease with increasing SDTA especially when the delay budget is large, which is shown by Fig. 14(a). In contrast, the achievable utility is nearly constant over varying SDTA even for a large delay budget [as shown in Fig. 14(b)], because proposed fuzzy path model can actively adapt to different degrees of directional correlation.

In Fig. 15, more details of the comparison are given for a relative large delay budget (3000 s in this case). For the scheme without prediction, only immediate neighboring

[4]The percentage of delivery tasks which are accomplished within delay budget.

TABLE VI
SIMULATION PARAMETERS FOR NODE SELECTION

Parameters	Values
Network Area	10000*10000 metres
Transmission Range	750 metres
Number of Stationary Nodes	21*21
Deployment of Stationary Nodes	uniformly distributed
Gateway Location	bottom right corner
Routing Algorithm	position-based greedy
Original Position	random within network area
Initial Direction	random within $[-\pi, \pi]$
Number of Delivery Tasks	1000

nodes can be selected as the relay and therefore the utility is constant and does not change with the SDTA. For the scheme based on linear trajectory model, the utility decreases with increasing SDTA due to lower delivery ratio caused by more randomness in movement. Because of the large delay budget, the linear trajectory model is no longer accurate for contact prediction so that the achieved utility is always worse than the scheme without prediction. With the proposed fuzzy path model, higher achievable utility can be realized because of its dynamic reaction to the movement directivity.

As shown in Fig. 15, the delivery utility achieved by the proposed fuzzy path model is related to the threshold[5] of certainty degree (i.e., the minimum required contact certainty to qualify a set of stationary nodes as relay candidates). With increasing certainty threshold, the utility achieved by the fuzzy path model approximates the scheme without prediction, due to lower allowed uncertainty. By filtering out unqualified candidates (i.e., stationary nodes who do not have enough contact certainty), the proposed fuzzy path model can always outperform the linear trajectory model when the threshold value is no less than 0.6. For the performance at the threshold value 0.6, the delivery utility increases after a certain SDTA value (15° in this case) because there is no more opportunistic forwarding when the movement becomes less predictable. With a higher threshold (no less than 0.8 in this case), its performance is always no worse than the scheme without prediction, owing to the relay selection from a more appropriate set of candidates.

Compared with the zero allowance of uncertainty (i.e., a threshold value of 1), a moderate uncertainty threshold (i.e., a value 0.8 in this case) can achieve higher utility because it tends to identify better relay candidates (who have fewer forwarding hops whilst keeping a low enough risk of delivery failure). Even when the threshold value equals to one, the utility achieved by the proposed scheme can be higher than the scheme without prediction when the SDTA is very small (5° in this case), as the directivity of movement is strong enough to provide additional candidates without concerning uncertainty. Furthermore, although a higher achievable utility becomes less possible with increasing randomness (as the risk associated with opportunistic delivery increases), it is shown that the mobility with a moderate value of SDTA (less then 30° in this case) is exploitable as directional movement to facilitate packet forwarding.

[5]By this we mean a lower-bound degree value.

VI. CONCLUSION

In this paper, the feasible exploitation of directional movement in path-unconstrained mobility is investigated for strategic forwarding. The state-of-the-art forwarding schemes are studied and the related literature is reviewed. The main contribution of our research is a systematic framework for analytical modeling of relay selection. Considering current limitations, a novel fuzzy path model is proposed for movement estimation, where the influence of directional correlation is quantified by the SDTAs. Our proposal advances the state-of-the-art because the directional correlation of destination movement is considered to dynamically exploit the node mobility for the optimal selection of the stationary relay node. Simulation results show that higher delivery utility can be achieved by the proposed fuzzy path model, compared with a forwarding scheme without contact prediction or one based on linear trajectory prediction. As a conclusion, the directional movement is exploitable for the dissemination of delay-tolerant information especially when moderate uncertainty is allowed. Further research can be conducted to devise appropriate forwarding strategies in different scenarios.

REFERENCES

[1] A. Cerpa *et al.*, "Habitat monitoring: Application driver for wireless communications technology," *ACM SIGCOMM Comput. Commun. Rev.*, vol. 31, no. S2, pp. 20–41, 2001.

[2] J. Ahn *et al.*, "WildSense: Monitoring interactions among wild deer in harsh outdoor environments using a delay-tolerant WSN," *J. Sensors*, vol. 2016, Jul. 2016, Art. no. 1693460. [Online]. Available: https://www.hindawi.com/journals/js/2016/1693460/cta/

[3] A. Mainwaring, D. Culler, J. Polastre, R. Szewczyk, and J. Anderson, "Wireless sensor networks for habitat monitoring," in *Proc. ACM 1st ACM Int. Workshop Wireless Sensor Netw. Appl. (WSNA)*, Atlanta, GA, USA, 2002, pp. 88–97.

[4] I. F. Akyildiz, D. Pompili, and T. Melodia, "Underwater acoustic sensor networks: Research challenges," *Ad Hoc Netw.*, vol. 3, no. 3, pp. 257–279, 2005.

[5] I. F. Akyildiz and I. H. Kasimoglu, "Wireless sensor and actor networks: Research challenges," *Ad Hoc Netw.*, vol. 2, no. 4, pp. 351–367, 2004.

[6] B. Liu, T. Jiang, Z. Wang, and Y. Cao, "Object-oriented network: A named-data architecture toward the future Internet," *IEEE Internet Things J.*, vol. 4, no. 4, pp. 957–967, Aug. 2017.

[7] Y. Cao, T. Jiang, and Z. Han, "A survey of emerging M2M systems: Context, task, and objective," *IEEE Internet Things J.*, vol. 3, no. 6, pp. 1246–1258, Dec. 2016.

[8] L. Gou, G. Zhang, D. Bian, W. Zhang, and Z. Xie, "Data dissemination in wireless sensor networks with instantly decodable network coding," *J. Commun. Netw.*, vol. 18, no. 5, pp. 846–856, Oct. 2016.

[9] M. T. Nuruzzaman and H.-W. Ferng, "A low energy consumption routing protocol for mobile sensor networks with a path-constrained mobile sink," in *Proc. IEEE Int. Conf. Commun. (ICC)*, Kuala Lumpur, Malaysia, May 2016, pp. 1–6.

[10] G.-L. Chiou, S.-R. Yang, and W.-T. Yen, "On trajectory-based I2V group message delivery over vehicular ad-hoc networks," *IEEE Trans. Veh. Technol.*, vol. 65, no. 9, pp. 7389–7402, Sep. 2016.

[11] R. Kim, H. Lim, and B. Krishnamachari, "Prefetching-based data dissemination in vehicular cloud systems," *IEEE Trans. Veh. Technol.*, vol. 65, no. 1, pp. 292–306, Jan. 2016.

[12] C.-M. Yu, C.-S. Lu, and S.-Y. Kuo, "Habitual behavior-based opportunistic data forwarding in wildlife tracking," in *Proc. IEEE 4th Int. Symp. Wireless Commun. Syst.*, Trondheim, Norway, 2007, pp. 807–808.

[13] C. Liu and J. Wu, "Scalable routing in cyclic mobile networks," *IEEE Trans. Parallel Distrib. Syst.*, vol. 20, no. 9, pp. 1325–1338, Sep. 2009.

[14] Y. Sun, J. Guo, and Y. Yao, "Speed up-greedy perimeter stateless routing protocol for wireless sensor networks (SU-GPSR)," in *Proc. IEEE 18th Int. Conf. High Perform. Switching Routing (HPSR)*, Campinas, Brazil, Jun. 2017, pp. 1–6.

[15] J. He, L. Cai, P. Cheng, and J. Pan, "Delay minimization for data dissemination in large-scale VANETs with buses and taxis," *IEEE Trans. Mobile Comput.*, vol. 15, no. 8, pp. 1939–1950, Aug. 2016.
[16] Y. Li, D. Jin, P. Hui, and S. Chen, "Contact-aware data replication in roadside unit aided vehicular delay tolerant networks," *IEEE Trans. Mobile Comput.*, vol. 15, no. 2, pp. 306–321, Feb. 2016.
[17] Y. Cao *et al.*, "Geographic-based spray-and-relay (GSaR): An efficient routing scheme for DTNs," *IEEE Trans. Veh. Technol.*, vol. 64, no. 4, pp. 1548–1564, Apr. 2015.
[18] K. Pandey, S. K. Raina, and R. S. Raw, "Distance and direction-based location aided multi-hop routing protocol for vehicular ad-hoc networks," *Int. J. Commun. Netw. Distrib. Syst.*, vol. 16, no. 1, pp. 71–98, Dec. 2016.
[19] X. Wu, K. N. Brown, and C. J. Sreenan, "Data pre-forwarding for opportunistic data collection in wireless sensor networks," *ACM Trans. Sensor Netw.*, vol. 11, no. 1, pp. 1–33, Nov. 2014.
[20] U. Sadiq and M. Kumar, "ProxiMol: Proximity and mobility estimation for efficient forwarding in opportunistic networks," in *Proc. IEEE 8th Int. Conf. Mobile Ad-Hoc Sensor Syst.*, Valencia, Spain, Oct. 2011, pp. 312–321.
[21] S. Batabyal and P. Bhaumik, "Mobility models, traces and impact of mobility on opportunistic routing algorithms: A survey," *IEEE Commun. Surveys Tuts.*, vol. 17, no. 3, pp. 1679–1707, 3rd Quart., 2015.
[22] B. Liang and Z. J. Haas, "Predictive distance-based mobility management for multidimensional PCS networks," *IEEE/ACM Trans. Netw.*, vol. 11, no. 5, pp. 718–732, Oct. 2003.
[23] M. Zhao and W. Wang, "WSN03-4: A novel semi-Markov smooth mobility model for mobile ad hoc networks," in *Proc. IEEE Globecom*, San Francisco, CA, USA, Nov. 2006, pp. 1–5.
[24] S. Bandyopadhyay, E. J. Coyle, and T. Falck, "Stochastic properties of mobility models in mobile ad hoc networks," *IEEE Trans. Mobile Comput.*, vol. 6, no. 11, pp. 1218–1229, Nov. 2007.
[25] L. Feng, Q. Zhao, and H. Zhang, "Location management based on distance and direction for PCS networks," *Comput. Netw.*, vol. 51, no. 1, pp. 134–152, Jan. 2007.
[26] Q. Zhao, S. C. Liew, S. Zhang, and Y. Yu, "Distance-based location management utilizing initial position for mobile communication networks," *IEEE Trans. Mobile Comput.*, vol. 15, no. 1, pp. 107–120, Jan. 2016.
[27] Z. J. Haas, "A new routing protocol for the reconfigurable wireless networks," in *Proc. 6th Int. Conf. Universal Pers. Commun. (ICUPC)*, vol. 2. San Diego, CA, USA, Oct. 1997, pp. 562–566.
[28] E. A. Codling, M. J. Plank, and S. Benhamou, "Random walk models in biology," *J. Roy. Soc. Interface*, vol. 5, no. 25, pp. 813–834, 2008.
[29] H.-I. Wu, B.-L. Li, T. A. Springer, and W. H. Neill, "Modelling animal movement as a persistent random walk in two dimensions: Expected magnitude of net displacement," *Ecol. Model.*, vol. 132, nos. 1–2, pp. 115–124, 2000.
[30] J. A. Byers, "Correlated random walk equations of animal dispersal resolved by simulation," *Ecology*, vol. 82, no. 6, pp. 1680–1690, 2001.
[31] P. Nouvellet, J. P. Bacon, and D. Waxman, "Fundamental insights into the random movement of animals from a single distance-related statistic," *Amer. Naturalist*, vol. 174, no. 4, pp. 506–514, 2009.
[32] B. N. Clark, C. J. Colbourn, and D. S. Johnson, "Unit disk graphs," *Discr. Math.*, vol. 86, nos. 1–3, pp. 165–177, Jan. 1991.
[33] B. Zhou, Q. Chen, and P. Xiao, "The error propagation analysis of the received signal strength-based simultaneous localization and tracking in wireless sensor networks," *IEEE Trans. Inf. Theory*, vol. 63, no. 6, pp. 3983–4007, Jun. 2017.
[34] H. Fischer, *A History of the Central Limit Theorem: From Classical to Modern Probability Theory* (Sources and Studies in the History of Mathematics and Physical Sciences). New York, NY, USA: Springer, 2010.
[35] R. Y. Rubinstein and D. P. Kroese, *Simulation and the Monte Carlo Method*, vol. 10. Hoboken, NJ, USA: Wiley, 2016.
[36] K. Sohraby, D. Minoli, and T. Znati, *Wireless Sensor Networks: Technology, Protocols, and Applications*. Hoboken, NJ, USA: Wiley, 2007.

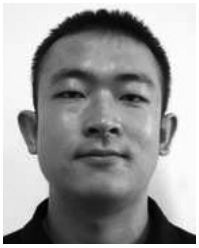

Yuhui Yao received the B.Eng. degree from the Beijing University of Posts and Telecommunications, Beijing, China, in 2014. He is currently pursuing the doctoral degree at the School of Electronic Engineering and Computer Science, Queen Mary University of London, London, U.K.

His current research interests include software-defined networking, Internet of Things, ad hoc networks, and mobility models.

Yan Sun received the B.Eng. degree in telecommunications engineering from the Beijing University of Posts and Telecommunications, Beijing, China, in 2001, and the M.Sc. and Ph.D. degrees in electronic engineering from the Queen Mary University of London, London, U.K., in 2003 and 2009, respectively.

In 2001, she joined Siemens Ltd., Beijing, as a Network Optimization Engineer, which she then rejoined as a System Engineer in research and development in 2003 and a Product Manager for five years. In 2009, she joined the Queen Mary University of London, as a Lecturer. Her current research interests include ad hoc networks, energy saving for modern mobile networks, software defined networks, and mobile healthcare networks.

Chris Phillips received the B.Eng. degree in telecommunications engineering in 1987 and Ph.D. degree in concurrent discrete event-driven simulation from the Queen Mary University of London, London, U.K.

He was then involved with research in industry for nine years as a Hardware and Systems Engineer with Bell Northern Research, Ottawa, ON, Canada, Siemens Roke Manor Research, Romsey, U.K., and Nortel Networks, Ottawa. In 2000, he returned to the Queen Mary University of London. His current research interests include broadband network protocols, resource management, and resilience.

Yue Cao (M'16) received the Ph.D. degree from the Institute for Communication Systems (ICS), University of Surrey, Guildford, U.K., in 2013.

He was a Research Fellow with ICS until 2016, and a Lecturer with the Department of Computer and Information Sciences, Northumbria University, Newcastle upon Tyne, U.K., until 2017, where he has been a Senior Lecturer since 2017. His current research interest includes intelligent mobility.

Dr. Cao is an Associate Editor for IEEE ACCESS.